Semnan University

Mechanics of Advanced Composite Structures

journal homepage: http://MACS.journals.semnan.ac.ir

Sensitivity Analysis of Vibrating Laminated Composite Rectangular Plates in Interaction with Inviscid Fluid Using EFAST Method

K. Khorshidi*, M. Taheri, M. Ghasemi

Department of Mechanical Engineering, Faculty of Engineering, Arak University, Arak, 38156-88349, Iran.

KEYWORDS

Vibration
Sensitivity analysis
Laminate composite plate
FSI
Inviscid fluid

ABSTRACT

This work investigates the sensitivity analysis of vibrating laminated composite rectangular plates in interaction with inviscid fluid using the modified higher-order shear deformation plate theory. The EFAST method which is based on variance and is independent of any assumption of linearity and uniformity between inputs and outputs is utilized for sensitivity analysis of laminated composite rectangular plates. Theoretical formulations, both for the laminated rectangular plates in interaction with inviscid, incompressible and irrotational fluid and the sensitivity analysis technique are summarized here. A Cartesian coordinate system is used to describe governing equations of fluid-structure interaction. Hamilton's variational principle is used to derive the Eigen problem of the complex system. A numerical investigation is carried out by using the Galerkin method and the boundary conditions of the plate are simply supported. A set of admissible displacement functions which satisfy identically the geometric boundary conditions are used to calculate the wet natural frequencies of the plate. In the numerical examples, the effect of the aspect ratio, thickness ratio and material orthotropy orientation of the plate, depth ratio and width of the fluid on the fundamental natural frequency of the vibrating laminated composite rectangular plates are examined and discussed.

1. Introduction

The extent to which a fluid can play a role in vibrational behavior of a structure continues to be an issue of interest to researchers. The existence of fluid around a structure changes the kinetic energy of the system and influences the natural frequencies and mode shapes[1, 2]. Hence, knowing about the dynamic response of the structure in contact with the fluid is necessary for various areas of engineering such as submarines, shipbuilding, nuclear, hydrodynamics and ocean engineering. Commonly, to analyze the frequency response of a structure in contact with a fluid is generally known as fluid-structure interaction (FSI). Widely analyzing FSI problems can be categorized into three methods: firstly, numerical methods such as the boundary element method and secondly, the fluid finite element method which needs a large number of computations and can be applied to numerous FSI problems [3-19]. In addition, sensitivity analysis (SA) investigates how the variation in the output of a numerical model can be attributed to variations of its input factors [20]. Sensitivity analysis is increasingly being used in environmental modeling for a variety of purposes, including uncertainty assessment, model calibration and diagnostic evaluation, dominant control analysis, and robust decision-making. Furthermore, sensitivity analysis is increase also being used in statics and dynamics modeling for a variety of scientific and engineering purposes, including vibrational behavior of structures, control analysis of systems, evaluation of material strengths in different conditions, etc. Numerous studies have been performed to investigate the sensitivity analysis of vibrating structures. Khedmati et al. [21] studied the sensitivity analysis of elastic buckling of a cracked plate with simply supported plates, subjected to an axial compressive edge load using the finite element method. Afonso and Hinton [22] used an automated approach to carry out sensitivity

* Corresponding author. Tel.: +98-863-2625720; Fax: +98-86-34173450
E-mail address: k-khorshidi@araku.ac.ir

DOI: 10.22075/MACS.2020.18605.1224
Received 2019-09-03; Received in revised form 2020-01-28; Accepted 2020-01-28

analysis and to obtain optimum shapes for plates and shells in which the natural frequencies were maximized. Akoussan et al. [23] proposed a high order continuous sensitivity analysis of the damping properties of viscoelastic composite plates according to their layers thicknesses. Chen and Tan[24], Fung and Chen [25], and Chen and Hsu [26], employing Galerkin and the Runge–Kutta method, presented the imperfection sensitivity of nonlinear vibration of a simply supported ceramic/metal functionally graded plate in a general state of arbitrary initial stresses. Łasecka-Plura and Lewandowski [27], using Euler-Bernoulli theory considered the sensitivity analysis of dynamic characteristics of composite beams with viscoelastic layers. In this study, the fractional Zener model was used to express the viscoelastic material properties.in another study, Kotełko et al. [28], presented a sensitivity analysis of thin-walled box-section girders subjected to pure bending based on the methodology of the Monte-Carlo method. Lima et al. [29], also developed the formulation of first-order sensitivity analysis of complex frequency response functions (FRFs) for composite sandwich plates composed by a combination of fiber-reinforced and elastomeric viscoelastic layers, in arrangements that were frequently used for noise and vibration attenuation. Research by Takezawa and Kitamura [30] studied the sensitivity analysis of objective functions including the eigenmodes of continuum systems using scalar Helmholtz equations. Additionally, Li et al. [31] proposed the sensitivity-analysis of vibro-acoustic systems by using the interval perturbation method compared with the Monte Carlo method. Li and Liu [32], developed a three-dimensional semi-analytical model for the static response and sensitivity analysis of the composite stiffened laminated plate with interfacial imperfections. Li et al. [33], investigated the free vibration analysis and eigenvalues sensitivity analysis of composite laminates with interfacial imperfection based on the radial point interpolation method (RPIM) in the Hamilton system. Liu [34], described an analytical method to calculate the sensitivity of the frequencies and modes with respect to fiber Vol. fractions and orientations, for the large-scale composite laminated structures with complex boundaries. Furthermore, Hu et al. [35], studied an explicit time-domain method for sensitivity analysis of structural responses under non-stationary random excitations. Yan and Cheng [36], analyzed the sensitivity of residual vibrations of structures subject to impacts using an adjoint method. In other publications, Choi and Byun [37], presented an effective sensitivity analysis algorithm for free vibration of a rectangular plate structure by using the finite element-transfer stiffness coefficient method. Liu and Paavola [38] also described a general analytical sensitivity analysis method for the composite laminated plates and shells, which was applied to both classical and first-order shear deformation theories and based on the finite element methods. Li et al. [39], studied the linear statics and free vibration sensitivity analysis of the composite sandwich plates based on a layerwise/solid-element method (LW/SE).

The main purpose of this paper is to present an analytical model for sensitivity analysis of vibrating laminated composite rectangular plates in interaction with inviscid fluid using modified higher-order shear deformation plate theory. Various plate theories are used to model the structure. Governing equations are derived using Hamilton's principle and solved with the Galerkin method. Using the EFAST method sensitivity of fundamental natural frequency is obtained. After validation, influences of the aspect ratio, thickness ratio and material orthotropy orientation of the plate, depth ratio and width of the fluid on the wet fundamental natural frequencies of the plate are illustrated.

2. Constitutive equation and modified shear deformation plate theory

Consider a laminated composite rectangular plate with length a, width b, total thickness h, and k elastic orthotropic layers, which is a part of the vertical side of a bounded rigid tank filled with a fluid, as shown in Fig. 1. The tank contains fluid that has width c_1, depth b_1 and mass density of fluid ρ_F. The fluid is considered incompressible, inviscid and irrotational. A Cartesian coordinate system is used to describe governing equations. The coordinate system is placed so that the origin is located in the corner of the studied plate on its middle surface, while axes x and y lie on the plate's edges and axis z is perpendicular to the middle plane.

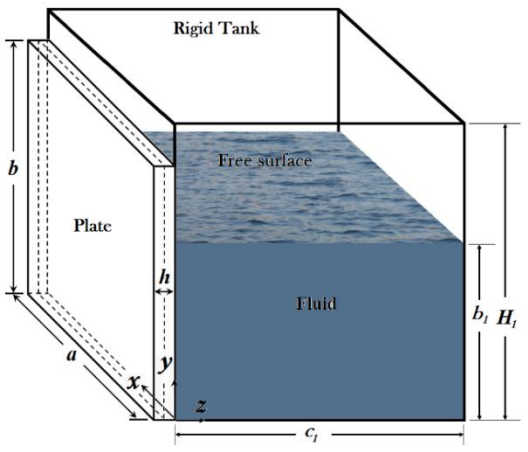

Fig. 1. Plate-fluid interaction, Coordinates and dimensions

The constitutive equations for k-th orthotropic lamina of the plate, in the material principal coordinates, under the hypothesis $\sigma_{zz} = 0$, are given by:

$$\begin{Bmatrix} \sigma_{xx} \\ \sigma_{yy} \\ \tau_{yz} \\ \tau_{xz} \\ \tau_{xy} \end{Bmatrix}^{(k)} = \begin{bmatrix} Q_{11} & Q_{12} & 0 & 0 & 0 \\ Q_{21} & Q_{22} & 0 & 0 & 0 \\ 0 & 0 & Q_{44} & 0 & 0 \\ 0 & 0 & 0 & Q_{55} & 0 \\ 0 & 0 & 0 & 0 & Q_{66} \end{bmatrix}^{(k)} \begin{Bmatrix} \varepsilon_{xx} \\ \varepsilon_{yy} \\ \gamma_{yz} \\ \gamma_{xz} \\ \gamma_{xy} \end{Bmatrix} \quad (1)$$

where superscript (k) refers to the k-th layer within a laminate, σ_{ij} and ε_{ij} are the normal stresses and strains, respectively, τ_{ij} and γ_{ij} are the shear stresses and strains, respectively, and Q_{ij}s are transformed material constants and defined by

$$[Q]^{(k)} = [T^{-1}C(T^{-1})^T]^{(k)} \quad (2)$$

in which:

$$\mathbf{T} = \begin{bmatrix} \cos^2\theta & \sin^2\theta & 0 & 0 & 2\cos\theta\sin\theta \\ \sin^2\theta & \cos^2\theta & 0 & 0 & -2\cos\theta\sin\theta \\ 0 & 0 & \cos\theta & -\sin\theta & 0 \\ 0 & 0 & \sin\theta & \cos\theta & 0 \\ -\cos\theta\sin\theta & \cos\theta\sin\theta & 0 & 0 & \cos^2\theta - \sin^2\theta \end{bmatrix} \quad (3)$$

$$\mathbf{C} = \begin{bmatrix} c_{11} & c_{12} & 0 & 0 & 0 \\ c_{21} & c_{22} & 0 & 0 & 0 \\ 0 & 0 & G_{23} & 0 & 0 \\ 0 & 0 & 0 & G_{13} & 0 \\ 0 & 0 & 0 & 0 & G_{12} \end{bmatrix} \quad (4)$$

where θ is the lamina material orthotropy orientation, G_{12}, G_{13} and G_{23} are the shear moduli in 1-2, 1-3 and 2-3 directions, respectively, and the coefficients c_{ij} are given by

$$c_{11} = \frac{E_1}{1 - \nu_{12}\nu_{21}}$$

$$c_{12} = c_{21} = \frac{E_2\nu_{12}}{1 - \nu_{12}\nu_{21}} \quad (5)$$

$$c_{22} = \frac{E_2}{1 - \nu_{12}\nu_{21}}$$

$$\nu_{ij}E_j = \nu_{ji}E_i$$

Equation (1) is obtained (i) under the transverse isotropy assumption with respect to planes parallel to the 2-3 plane, i.e., assuming fibers in the direction parallel to axis 1, so that $E_2 = E_3$, $G_{12} = G_{13}$ and $\nu_{12} = \nu_{13}$, and (ii) solving the constitutive equations for ε_{zz} as function of ε_{xx} and ε_{yy} and then eliminating it. Three independent displacements variables u_0, v_0 and w_0 in x, y and z directions, respectively, are used to describe middle surface deformations of the plate. The displacements u_x, u_y, u_z of a generic point of the plate at distance z from the $z = 0$ plane (see Fig.1) are related to the middle surface displacements u_0, v_0 and w_0 by:

$$u_x(x,y,z,t) = u_0(x,y,t) - \left(z + \frac{h}{2}\right)\frac{\partial w_0(x,y,t)}{\partial x} + f_1\left(z + \frac{h}{2}\right)\varphi_x(x,y,t) \quad (6)$$

$$u_y(x,y,z,t) = v_0(x,y,t)\left(z + \frac{h}{2}\right)\frac{\partial w_0(x,y,t)}{\partial y} + f_1\left(z + \frac{h}{2}\right)\varphi_y(x,y,t) \quad (7)$$

$$u_z(x,y,z,t) = w_0(x,y,t) \quad (8)$$

where φ_x and φ_y are the rotations of the transverse normals about the y and x axes, respectively, and $f_1(z)$ for exponential, trigonometric and hyperbolic shear deformation plate theories are given by

$$f_1(z + h/2) = (z + h/2)e^{-2\left(\frac{z}{h}+1/2\right)^2} \quad \text{Exponential SDPT} \quad (9)$$

$$f_1(z + h/2) = \frac{h}{\pi}\sin\left(\pi(\frac{z}{h} + 1/2)\right) \quad \text{Trigonometric SDPT} \quad (10)$$

$$f_1(z + h/2) = h\sinh\left(\frac{z}{h} + 1/2\right) - (z + h/2)\cosh(1/2) \quad \text{Hyperbolic SDPT} \quad (11)$$

The linear strain-displacement equations for the modify higher order shear deformation plate theory are given by

$$\varepsilon_{xx} = \frac{\partial u_x}{\partial x} = \frac{\partial u_0}{\partial x} - (z + h/2)\frac{\partial^2 w_0}{\partial x^2} + f_1(z + h/2)\frac{\partial \varphi_x}{\partial x} \quad (12)$$

$$\varepsilon_{yy} = \frac{\partial u_y}{\partial y} = \frac{\partial v_0}{\partial y} - (z + h/2)\frac{\partial^2 w_0}{\partial y^2} + f_1(z + h/2)\frac{\partial \varphi_y}{\partial y} \quad (13)$$

$$\gamma_{xy} = \left(\frac{\partial u_x}{\partial y} + \frac{\partial u_y}{\partial x}\right) = \left(\frac{\partial u_0}{\partial y} + \frac{\partial v_0}{\partial x}\right) - 2(z + h/2)\frac{\partial^2 w_0}{\partial x \partial y} + f_1(z + h/2)\left(\frac{\partial \varphi_x}{\partial y} + \frac{\partial \varphi_y}{\partial x}\right) \quad (14)$$

$$\gamma_{xz} = \left(\frac{\partial u_x}{\partial z} + \frac{\partial u_z}{\partial x}\right) = \varphi_x \frac{\partial f_1(z + h/2)}{\partial z} \quad (15)$$

$$\gamma_{yz} = \left(\frac{\partial u_z}{\partial y} + \frac{\partial u_y}{\partial z}\right) = \varphi_y \frac{\partial f_1(z + h/2)}{\partial z}. \quad (16)$$

The elastic strain U_p and kinetic T_p energies of the plate, including rotary inertia, are given by

$$U_p = \frac{1}{2}\sum_{k=1}^{K}\int_0^b\int_0^a\int_{h^{(k-1)}}^{h^{(k)}} \left(\sigma_{xx}^{(k)}\varepsilon_{xx} + \sigma_{yy}^{(k)}\varepsilon_{yy} + \sigma_{xy}^{(k)}\gamma_{xy} + \sigma_{xz}^{(k)}\gamma_{xz} + \sigma_{yz}^{(k)}\gamma_{yz}\right)\mathrm{dz\ dx\ dy} \quad (17)$$

$$T_p = \frac{1}{2}\sum_{k=1}^{K}\int_0^b\int_0^a\int_{h^{(k-1)}}^{h^{(k)}} \rho_p^{(k)}\left((\dot{u}_x)^2 + (\dot{u}_y)^2 + (\dot{u}_z)^2\right)\mathrm{dz\ dx\ dy} \quad (18)$$

where $\rho_p^{(k)}$ is the mass density of the k-th layer of the plate and the overdot denotes time derivative. The total kinetic energy of the fluid with respect to the bulging modes of the plate and the fluid sloshing can be written[1, 2]

$$T_{fB} = -\frac{1}{2}\rho_F\int_0^a\int_0^{b_1}\Phi_B(x,y,0,t)\frac{\partial \mathrm{v}(x,y,t)}{\partial t}\mathrm{dydx} \quad (19)$$

$$T_{fS} = -\frac{1}{2}\rho_F\int_0^a\int_0^{b_1}\Phi_S(x,y,0,t)\frac{\partial w_0(x,y,t)}{\partial t}\mathrm{dydx} \quad (20)$$

where Φ_B and Φ_S are fluid potential velocity relating to bulging modes and sloshing modes, respectively.

$$\phi_B(x,y,z,t) = \sum_{l_1=0}^{\infty}\sum_{k_1=0}^{\infty} A_{l_1,k_1}(t)\cos\left(\frac{l_1\pi x}{a}\right) h\left(\frac{(2k_1+1)\pi y}{2b_1}\right)\left(e^{S_1 z} + e^{S_1(2c_1 - z)}\right) \quad (21)$$

$$S_1 = \pi\sqrt{(l_1/a)^2 + (2k_1 + 1/(2b_1))^2}$$

$$(l_1 = k_1 = 0,1,2,\dots)$$

$$\phi_S(x,y,z,t) = \sum_{i_1=0}^{N_s}\sum_{j_1=0}^{M_s} B_{i_1,j_1}(t)\cos\left(\frac{i_1\pi x}{a}\right)\cosh(S_2 y)\cos\left(\frac{j_1\pi z}{c_1}\right) \quad (22)$$

$$S_2 = \pi\sqrt{(i_1/a)^2 + (j_1/c_1)^2}$$

$$(i_1 = j_1 = 0,1,2\dots)$$

where $B_{i_1,j_1}(t)$ is the unknown coefficients related to fluid sloshing; N_s and M_s express the number of necessary terms to get desirable accuracy. Furthermore, $A_{l_1,k_1}(t)$ are Fourier coefficients associated with the bulging modes

$$A_{l_1,k_1}(t) = \frac{\frac{coff}{ab_1}\int_0^a\int_0^{b_1}\frac{\partial w(x,y,t)}{\partial t}\cos\left(\frac{l_1\pi x}{a}\right)\cos\left(\frac{(2k_1+1)\pi y}{2b_1}\right)\mathrm{dydx}}{S_1(1 - e^{S_1(2c_1)})}$$

$$coff = \begin{cases} 1 & if\ \ l_1 = k_1 = 0 \\ 2 & if\ \ l_1 or\ k_1 = 0 \\ 4\ if\ l_1\ and\ k_1 = 0 \end{cases} \quad (23)$$

i_1, j_1, l_1 and k_1 are nonnegative integers. Moreover, Using the assumption of linearized sloshing [1, 2] at the free surface of fluid leads to

$$\rho_F\frac{\partial \Phi_B}{\partial y}\bigg|_{y=b_1} + \rho_F\frac{\partial \Phi_S}{\partial y}\bigg|_{y=b_1} - \rho_F\frac{\omega^2}{g}\Phi_S\bigg|_{y=b_1} = 0 \quad (24)$$

In which g is the acceleration of gravity and ω is the wet natural frequency of plate-fluid interaction.

3. Governing equations of fluid-structure

Hamilton's principle is employed to obtain the governing equations and associated boundary conditions of the system as follows

$$\int_0^t(\delta T_p + \delta T_{fS} + \delta T_{fB} - \delta U_p)dt = 0 \quad (25)$$

In which δ is variation operator. Now by inserting Eqs. (17), (18), (19) and (20) into Eq. (25) and then integrating by parts and setting the coefficients of δu_0, δv_0, δw_0, $\delta\varphi_x$ and $\delta\varphi_y$ to zero, boundary conditions and governing equations in terms of stress resultants can be derived as follows

$$\Gamma_1(u_0,v_0,w_0,\varphi_x,\varphi_y) = A_1\frac{\partial^2 u_0}{\partial x^2} + \quad (26)$$

$$A_3\frac{\partial^2\varphi_x}{\partial x^2}+A_4\frac{\partial^2 v_0}{\partial x\partial y}+A_6\frac{\partial^2\varphi_y}{\partial x\partial y}+A_7\frac{\partial^2 u_0}{\partial y^2}+A_9\frac{\partial^2\varphi_x}{\partial y^2}+A_7\frac{\partial^2 v_0}{\partial x\partial y}+A_9\frac{\partial^2\varphi_y}{\partial x\partial y}-A_2\frac{\partial^3 w_0}{\partial x^3}-A_5\frac{\partial^3 w_0}{\partial x\partial y^2}-2A_8\frac{\partial^3 w_0}{\partial y^2\partial x}-\left(I_1\frac{\partial^2 u_0}{\partial t^2}+I_4\frac{\partial^2\varphi_x}{\partial t^2}-I_2\frac{\partial^3 w_0}{\partial x\partial t^2}\right)$$

$$\Gamma_2(u_0,v_0,w_0,\varphi_x,\varphi_y)=A_1\frac{\partial^2 v_0}{\partial y^2}+A_3\frac{\partial^2\varphi_y}{\partial y^2}+A_4\frac{\partial^2 u_0}{\partial x\partial y}+A_6\frac{\partial^2\varphi_x}{\partial x\partial y}+A_7\frac{\partial^2 v_0}{\partial x^2}+A_9\frac{\partial^2\varphi_y}{\partial x^2}+A_7\frac{\partial^2 u_0}{\partial x\partial y}+A_9\frac{\partial^2\varphi_x}{\partial x\partial y}-A_2\frac{\partial^3 w_0}{\partial y^3}-A_5\frac{\partial^3 w_0}{\partial y\partial x^2}-2A_8\frac{\partial^3 w_0}{\partial x^2\partial y}-\left(I_1\frac{\partial^2 v_0}{\partial t^2}+I_4\frac{\partial^2\varphi_y}{\partial t^2}-I_2\frac{\partial^3 w_0}{\partial y\partial t^2}\right) \quad (27)$$

$$\Gamma_3(u_0,v_0,w_0,\varphi_x,\varphi_y.\Phi_S)=-A_{10}\frac{\partial^4 w}{\partial x^4}+A_{11}\frac{\partial^3\varphi_x}{\partial x^3}-A_{12}\frac{\partial^4 w_0}{\partial y^2\partial x^2}+A_{13}\frac{\partial^3\varphi_y}{\partial x^2\partial y}-A_{12}\frac{\partial^4 w_0}{\partial y^2\partial x^2}+A_{13}\frac{\partial^2\varphi_x}{\partial y^2\partial x}-A_{10}\frac{\partial^4 v_0}{\partial y^4}+A_{11}\frac{\partial^3\varphi_y}{\partial y^3}+2A_{15}\frac{\partial^3\varphi_x}{\partial y^2\partial x}-4A_{14}\frac{\partial^4 w_0}{\partial y^2\partial x^2}+2A_{15}\frac{\partial^3\varphi_y}{\partial x^2\partial y}+A_2\frac{\partial^3 u_0}{\partial x^3}+A_5\frac{\partial^3 v_0}{\partial x^2\partial y}+A_5\frac{\partial^3 u_0}{\partial y^2\partial x}+A_2\frac{\partial^3 v_0}{\partial y^3}+2A_8\frac{\partial^3 u_0}{\partial y^2\partial x}+2A_8\frac{\partial^3 v_0}{\partial x^2\partial y}-\left(-\frac{1}{2}\rho_F\left(\Phi_B(x,y,0,t)+\Phi_S(x,y,0,t)\right)+I_1\frac{\partial^2 w_0}{\partial t^2}+I_5\frac{\partial^3\varphi_y}{\partial y\partial t^2}+I_2\frac{\partial^3 v_0}{\partial y\partial t^2}-I_3\frac{\partial^4 w_0}{\partial y^2\partial t^2}+I_5\frac{\partial^3\varphi_x}{\partial x\partial t^2}+I_2\frac{\partial^3 u_0}{\partial x\partial t^2}-I_3\frac{\partial^4 w_0}{\partial x^2\partial t^2}\right) \quad (28)$$

$$\Gamma_4(u_0,v_0,w_0,\varphi_x,\varphi_y)=A_3\frac{\partial^2 u_0}{\partial x^2}+A_{16}\frac{\partial^2\varphi_x}{\partial x^2}+A_6\frac{\partial^2 v_0}{\partial x\partial y}+A_{17}\frac{\partial^2\varphi_y}{\partial x\partial y}+A_9\frac{\partial^2 u_0}{\partial y^2}+A_{18}\frac{\partial^2\varphi_x}{\partial y^2}+A_9\frac{\partial^2 v_0}{\partial x\partial y}+A_{18}\frac{\partial^2\varphi_y}{\partial x\partial y}-A_{11}\frac{\partial^3 w_0}{\partial x^3}-A_{13}\frac{\partial^3 w_0}{\partial x\partial y^2}-2A_{15}\frac{\partial^3 w_0}{\partial y^2\partial x}-A_{19}\varphi_x-\left(I_6\frac{\partial^2\varphi_x}{\partial t^2}+I_4\frac{\partial^2 u_0}{\partial t^2}-I_5\frac{\partial^3 w_0}{\partial x\partial t^2}\right) \quad (29)$$

$$\Gamma_5(u_0,v_0,w_0,\varphi_x,\varphi_y)=A_3\frac{\partial^2 v_0}{\partial y^2}+A_{16}\frac{\partial^2\varphi_y}{\partial y^2}+A_6\frac{\partial^2 u_0}{\partial x\partial y}+A_{17}\frac{\partial^2\varphi_x}{\partial x\partial y}+A_9\frac{\partial^2 v_0}{\partial x^2}+A_{18}\frac{\partial^2\varphi_y}{\partial x^2}+A_9\frac{\partial^2 u_0}{\partial x\partial y}+A_{18}\frac{\partial^2\varphi_x}{\partial x\partial y}-A_{11}\frac{\partial^3 w_0}{\partial y^3}-A_{13}\frac{\partial^3 w_0}{\partial y\partial x^2}-2A_{15}\frac{\partial^3 w_0}{\partial x^2\partial y}-A_{19}\varphi_y-\left(I_4\frac{\partial^2 v_0}{\partial t^2}+I_6\frac{\partial^2\varphi_y}{\partial t^2}-I_5\frac{\partial^3 w_0}{\partial y\partial t^2}\right) \quad (30)$$

$$\Gamma_6(w_0,\Phi_S)=\rho_F\frac{\partial\Phi_B}{\partial y}\Big|_{y=b_1}+\rho_F\frac{\partial\Phi_S}{\partial y}\Big|_{y=b_1}-\rho_F\frac{\omega^2}{g}\Phi_S\Big|_{y=b_1} \quad (31)$$

where

$$\{I_1,I_2,I_3,I_4,I_5,I_6\}=\sum_{k=1}^{K}\int_{h^{(k-1)}}^{h^{(k)}}\rho_p^{(k)}\left(1,\left(z+\frac{h}{2}\right),\left(z+\frac{h}{2}\right)^2,f_1\left(z+\frac{h}{2}\right),\left(z+\frac{h}{2}\right)f_1\left(z+\frac{h}{2}\right),f_1\left(z+\frac{h}{2}\right)^2\right)\mathrm{dz} \quad (32\text{-}37)$$

$$\{A_1,A_2,A_{10},A_3,A_{11},A_{16}\}=\sum_{k=1}^{K}\int_{h^{(k-1)}}^{h^{(k)}}Q_{11}\left(1,\left(z+\frac{h}{2}\right),\left(z+\frac{h}{2}\right)^2,f_1\left(z+\frac{h}{2}\right),\left(z+\frac{h}{2}\right)f_1\left(z+\frac{h}{2}\right),f_1\left(z+\frac{h}{2}\right)^2\right)\mathrm{dz} \quad (38\text{-}43)$$

$$\{A_4,A_5,A_{12},A_6,A_{13},A_{17}\}=\sum_{k=1}^{K}\int_{h^{(k-1)}}^{h^{(k)}}Q_{12}\left(1,\left(z+\frac{h}{2}\right),\left(z+\frac{h}{2}\right)^2,f_1\left(z+\frac{h}{2}\right),\left(z+\frac{h}{2}\right)f_1\left(z+\frac{h}{2}\right),f_1\left(z+\frac{h}{2}\right)^2\right)\mathrm{dz} \quad (44\text{-}49)$$

$$\{A_7,A_8,A_{14},A_9,A_{15},A_{18}\}=\sum_{k=1}^{K}\int_{h^{(k-1)}}^{h^{(k)}}Q_{12}\left(1,\left(z+\frac{h}{2}\right),\left(z+\frac{h}{2}\right)^2,f_1\left(z+\frac{h}{2}\right),\left(z+\frac{h}{2}\right)f_1\left(z+\frac{h}{2}\right),f_1\left(z+\frac{h}{2}\right)^2\right)\mathrm{dz} \quad (50\text{-}55)$$

$$A_{19}=\sum_{k=1}^{K}\int_{h^{(k-1)}}^{h^{(k)}}Q_{66}\left(\frac{\partial f_1(z+h/2)}{\partial z}\right)^2\mathrm{dz} \quad (60)$$

4. Solution procedure using Galerkin approach

Governing equation systems (26)-(30) cannot be solved unless unknown coefficients $B_{i_1,j_1}(t)$ are determined. Hence, linear sloshing equation (31) must be added to Eqs. (26)-(30) as the seventh equation. For the sake of simplicity, the left-hand side of Eqs. (26)-(31) are denoted as Γ_i (i=1,2,..6) respectively. So applying the Galerkin method to Eqs. (26)-(31) leads to

$$\int_0^b \int_0^a \Gamma_1(u_0,v_0,w_0,\varphi_x,\varphi_y)u_0(x,y)\mathrm{dx\,dy} = 0 \quad (61)$$

$$\int_0^b \int_0^a \Gamma_2(u_0,v_0,w_0,\varphi_x,\varphi_y)v_0(x,y)\mathrm{dxdy} = 0 \quad (62)$$

$$\int_0^b \int_0^a \Gamma_3(u_0,v_0,w_0,\varphi_x,\varphi_y,\Phi_S)w_0(x,y)\mathrm{dxdy} = 0 \quad (63)$$

$$\int_0^b \int_0^a \Gamma_4(u_0,v_0,w_0,\varphi_x,\varphi_y)\varphi_x(x,y)\mathrm{dxdy} = 0 \quad (64)$$

$$\int_0^b \int_0^a \Gamma_5(u_0,v_0,w_0,\varphi_x,\varphi_y)\varphi_y(x,y)\mathrm{dxdy} = 0 \quad (65)$$

$$\int_0^c \int_0^a \Gamma_6(w,\Phi_S)\Phi_S|_{y=b_1}\mathrm{dx\,dz} = 0 \quad (66)$$

According to the Galerkin method, unknown functions of u_0, v_0, w_0, φ_x and φ_y propose in the following form

$$u_0(x,y,t) = \sum_{n=1}^{N}\sum_{m=1}^{M} u_{m,n}\bar{\bar{u}}_0(x,y)e^{i\omega t} \quad (67)$$

$$v_0(x,y,t) = \sum_{n=1}^{N}\sum_{m=1}^{M} v_{m,n}\bar{\bar{v}}_0(x,y)e^{i\omega t} \quad (68)$$

$$w_0(x,y,t) = \sum_{n=1}^{N}\sum_{m=1}^{M} w_{m,n}\bar{\bar{w}}_0(x,y)e^{i\omega t} \quad (69)$$

$$\varphi_x(x,y,t) = \sum_{n=1}^{N}\sum_{m=1}^{M} \varphi x_{m,n}\bar{\bar{\varphi}}_x(x,y)e^{i\omega t} \quad (70)$$

$$\varphi_y(x,y,t) = \sum_{n=1}^{N}\sum_{m=1}^{M} \varphi y_{m,n}\bar{\bar{\varphi}}_y(x,y)\,e^{i\omega t} \quad (71)$$

where M and N indicate truncated orders of series. $u_{m,n}$, $v_{m,n}$, $w_{m,n}$, $\varphi x_{m,n}$ and $\varphi y_{m,n}$ are undetermined coefficients which are calculated after minimizing residuals. $\bar{\bar{u}}_0(x,y)$, $\bar{\bar{v}}_0(x,y)$, $\bar{\bar{w}}_0(x,y)$, $\bar{\bar{\varphi}}_x(x,y)$ and $\bar{\bar{\varphi}}_y(x,y)$ are independent functions which satisfy at least essential boundary conditions. For simply supported boundary conditions$\bar{\bar{u}}_0(x,y)$, $\bar{\bar{v}}_0(x,y)$, $\bar{\bar{w}}_0(x,y)$, $\bar{\bar{\varphi}}_x(x,y)$ and $\bar{\bar{\varphi}}_y(x,y)$ can be written as

$$\bar{\bar{u}}_0(x,y) = \cos\left(\frac{m\pi x}{a}\right)\sin\left(\frac{n\pi y}{b}\right) \quad (72)$$

$$\bar{\bar{v}}_0(x,y) = \sin\left(\frac{m\pi x}{a}\right)\cos\left(\frac{n\pi y}{b}\right) \quad (73)$$

$$\bar{\bar{w}}_0(x,y) = \sin\left(\frac{m\pi x}{a}\right)\sin\left(\frac{n\pi y}{b}\right) \quad (74)$$

$$\bar{\bar{\varphi}}_x(x,y) = \sin\left(\frac{m\pi x}{a}\right)\cos\left(\frac{n\pi y}{b}\right) \quad (75)$$

$$\bar{\bar{\varphi}}_y(x,y) = \cos\left(\frac{m\pi x}{a}\right)\sin\left(\frac{n\pi y}{b}\right) \quad (76)$$

m and n are numbers of half-waves along x- and y- axis, respectively. After solving the above equations, one can find natural frequencies and mode shapes which are related to the eigenvalues and eigenfunctions of the system.

5. Sensitivity analysis

One of the parts of general sensitivity analysis techniques that has attracted more attention is the variance-based techniques. In these techniques, the sensitivity index is computed as the share of each parameter in the overall output variance of the model. The general sensitivity analysis techniques are implemented in four steps: (1) defining the inputs and the type of distribution of each input, (2) generating the samples for the input values, (3) computing the model's output for each set of input samples and (4) determining the effect of each input factor on the output [40]. In this section, the variance-based sensitivity analysis techniques have been reviewed. The variance-based general sensitivity analysis approaches can be used to obtain the first-order effect and the second-order effect (which include the interaction between other parameters) [41].

Moreover, the Sobol method [42] is a model-independent general sensitivity analysis technique which is based on variance analysis. This method can be used for nonlinear and non-uniform functions and models. For the model defined by function Y=f(x), where Y is the model output and X(x_1,x_2,…,x_n) is the vector of input parameters, Sobol' suggested to decompose the function f into summands of increasing dimensionality, where the integral of each term over its own input variables is zero. Sobol showed that, when all the inputs were perpendicular to one another, this resolution was unique and the output variance of the model (V) was the set of variances of each resolved term [42]:

$$V(Y)=\sum_{i=1}^{n} V_i + \sum_{i\le j\le 1}^{n} V_{ij}+\ldots+V_{1\ldots n} \quad (77)$$

In Eq. (77), V_i denotes the first-order effect for each input factor $x_i(V_i = V(E(Y|x_i)))$ and $V_{ij} = V\,(E\,(Y|x_i, x_j)) - V_i - V_j$ to $V_{1,\ldots,n}$ indicate the interactions between n factors. Therefore, the shares allocated to parameters, and the interactions of parameters can be determined from the total output variance. The sensitivity index is obtained as the ratio of each order's variance to the total variance variance ($S_i = V_i/V$denotes the first-order sensitivity index, $S_{ij} = V_{ij}/V$ represents the second-order sensitivity index, and so on). The total sensitivity index (i.e., the overall effect of each parameter) is obtained as the summand of all the orders of sensitivity index for that parameter [42]:

$$S_{Ti} = S_i + \sum_{i\neq j} S_{ij} + \cdots \quad (78)$$

The general equation has been presented by Sobol in 1990, which will be given as follows [43]:

$$\int_0^1 f_{i_1,..,i_s}\left(x_{i_1},\ldots,x_{i_s}\right)dx_{i_k} = o\ , \quad if\ 1\le k\le s \quad (79)$$

$$\int_{\Omega^k} f_{i_1\ldots,i_s} f_{j_1,..,j_l} dX = 0 \quad (80)$$

f_0 can be defined as:

$$f_0 = \int_{\Omega^k} f(X)dX \quad (81)$$

Sobol showed that all the terms of *f(X)* could be calculated through multiple integrals:

$$f_i(x_i) = -f_0 + \int_0^1 \ldots \int_0^1 f(X)dX_{\sim i} \quad (82)$$

$$f_{ij}\left(x_i.x_j\right) = -f_0 - f_i(x_i) + \int_0^1 \ldots \int_0^1 f(X)dX_{\sim ij} \quad (83)$$

Sensitivity index based on variance can be obtained as follows:

$$D = \int_{\Omega^k} f^2(X)dX - (f_0)^2 \quad (84)$$

In which D is the variance of $f(X)$.

Sensitivity value $s_{1,2,\ldots,k}$can be obtained by dividing of every group of variables variance to total variance.

It should be noted that any professional and official titles or academic degrees (Dr, chief, sir) must not show in Author details. In addition, first name should be written in abbreviation and family name in complete form.

$$s_{1,2,\ldots,k} = \frac{D_{1,2,\ldots,k}}{D} \quad for\ 1\le i_1<\cdots<i_s \le k \quad (85)$$

s_i is the first order sensitivity index for x_i factor which presents the sensitivity effect of x_i parameter on output and s_{ij} is the second order sensitivity index which shows the interaction effect on total variance.

$$\sum_{i=1}^{k} s_i + \sum_{1\le i<j\le k} s_{ij} + \cdots + s_{1,2,\ldots,k} = 1 \quad (86)$$

Total sensitivity index is a summation of all the sensitivity indices.

The EFAST method was presented by Cukier et al.[44] and was later improved by Saltelli et al. [45] Like the Sobol method, this approach is also based on variance and it is independent of any assumption of linearity and uniformity between inputs and output(s). Contrary to the Sobol method, which uses multidimensional integrals to obtain the total variance and the partial variances, this method converts the multidimensional integrals to one-dimensional ones by defining a transfer function and simplifies the procedure for the calculation of sensitivity indexes.

The EFAST method searches the n-dimensional space of the input factors (Unit Hypercube K^n) by using a Search Curve defined by a set of parametric equations [45]:

$$x_i = \frac{1}{2} + \frac{1}{\pi}\arcsin\left(sin(\omega_i s + \varphi_i)\right) \quad (87)$$

Where $\omega_i (i = 1,2,\ldots,n)$ is the frequency related to factor x_i, s is a variable that changes from –π to +π, and ϕ_i specifies the starting point of the curve. The output variance of the model is approximated by means of Fourier analysis:

$$\begin{aligned} V\,(Y) &= \frac{1}{2\pi}\int_{-\pi}^{\pi} f^2(s)ds - \left(\frac{1}{2\pi}\int_{-\pi}^{\pi} f(s)ds\right)^2 \\ &\approx \sum_{j=-\infty}^{\infty}(A_j^2+B_j^2) - (A_0^2+B_0^2) \\ &\approx 2\sum_{j=1}^{N}(A_j^2+B_j^2) \end{aligned} \quad (88)$$

In the above equation $f(s) = f\left(G_1(\sin(\omega_1 s)), G_2(\sin(\omega_2 s)), \ldots, G_n(\sin(\omega_n s))\right)$, G(s) are the transfer functions, and A_j and B_j are the Fourier coefficients $\left(A_j = \frac{1}{2\pi}\int_{-\pi}^{\pi} f(s)\cos(js)ds\right), B_j =$

$\frac{1}{2\pi}\int_{-\pi}^{\pi} f(s)\sin(js)\,ds$. By calculating the Fourier coefficients for the basic frequency (ω_i) and its higher harmonics ($p\omega_i$), the partial first-order input variance (x_i) can be obtained.

$$V_i = \sum_{p\in Z^0}(A^2_{p\omega_i} + B^2_{p\omega_i}) = 2\sum_{p=1}^{\infty}(A^2_{p\omega_i} + B^2_{p\omega_i}) \quad (89)$$

Also, like the Sobol method, the ratio of the first-order partial variance to total variance is used to compute the main sensitivity index. The total sensitivity index is obtained from Eq. (82)[46]:

$$ST_i = 1 - \frac{V_{-i}}{V} \quad (90)$$

variance V_{-i} is obtained by changing all the parameters except parameter x_i.

The Sobol method employs the Monte Carlo integral to obtain each partial variance; and in comparison, with the EFAST method, it does not use a transfer function; that is why, it has a low computational efficiency.

6. Numerical result

In this section, the wet natural frequency parameters are obtained from the Galerkin method for the free vibrations of a laminated composite rectangular plate interacting with the bounded fluid. Numerical results have been performed for simply supported boundary conditions. Materials chosen for the plate is graphite/epoxy with the material properties; Poisson's ratio $\nu_{12} = 0.25$, $\rho_p = 1000\ (\frac{\text{kg}}{\text{m}^3})$, $E_1 = 40$ GPa, $E_2 = 1$ GPa, $G_{12} = G_{13} = 0.6$ GPa and $G_{23} = 0.5$ GPa. Calculations have been performed for 4 layers symmetric laminated plates $(0^0/90^0/90^0/0^0)$. Presented results are obtained for the thickness ratios $h/a = 0.05 \rightarrow 0.2$, aspect ratios $a/b = 0.5 \rightarrow 5$, material orthotropy orientation $\theta = 0^0 \rightarrow 180^0$, depth of the fluid ratios $b_1/b = 0 \rightarrow 1$ and width of the tank $c_1 = 0 \rightarrow 10\,m$. Also, fluid density is considered as $\rho_F = 1000\ (\frac{\text{kg}}{\text{m}^3})$.

The comparison of the fundamental wet natural frequencies of the simply supported laminated composite plates obtained by Galerkin method are compared with those of Khorshidi and Farhadi [2] which are based on third order shear deformation plate theory (TSDT) and finite element analysis are presented in Table 1 for different thickness ratios including $h/a = 0.01$, 0.1 and 0.2. In Table 1, the numerical results are obtained for a four layer (0º/90º)s squared plate ($a = 1m, b = 1m, c_1 = 0.5\,m$)with different depth of the fluid (b_1/b) which is varies from 0 to 1. This comparison confirmed reliability of the proposed method and those that were presented by Khorshidi and Farhadi [2].

In this section, the effects of the various parameters such as aspect ratio (a/b), thickness ratio (h/a), material orthotropy orientation (θ), depth of the fluid ratio (b_1/b) and width of the tank (c_1) are illustrated in Figs. 2-6. according to the EFAST model that is used for sensitivity analysis, for each parameter in x-axis there exists several outputs in the y-axis because when a parameter has a particular value other parameter can be changed. For example, in Fig. 2 when the aspect ratio is equal to 1 other parameter such as thickness ratio (h/a) and... can be changed.

Figure. 2 illustrates the fundamental natural frequency versus the aspect ratios parameter. It is realized that aspect ratios parameter is the most sensitive parameter, since its changes have the steepest slope relative to other parameters.

Table 1. Comparison study of fundamental natural frequencies of a simply supported square laminated composite plate between analytical and FEM results.

$\frac{b_1}{b}$	$\frac{h}{a}=0.01$			$\frac{h}{a}=0.1$			$\frac{h}{a}=0.2$		
	Galekin	Rayleigh-Ritz [2]	FEM[2]	Galekin	Rayleigh-Ritz [2]	FEM [2]	Galekin	Rayleigh-Ritz [2]	FEM [2]
0	29.9696	29.9778	29.89544	240.427	240.440	239.2477	343.776	343.370	339.8131
0.1	29.6192	29.6885	29.50947	240.618	240.209	238.6906	343.696	343.207	341.7148
0.2	26.0108	26.0253	25.90472	235.806	236.976	233.9471	340.213	340.906	335.384
0.3	18.6970	18.6746	18.51837	226.655	225.097	224.3595	332.300	332.108	331.5882
0.4	13.0885	13.1129	12.96254	201.873	202.967	199.8331	313.840	313.689	313.5351
0.5	9.59987	9.5182	9.443441	176.281	176.190	174.5336	286.528	288.387	282.9549
0.6	7.35094	7.33229	7.230984	149.390	150.209	147.9097	256.077	257.746	256.7761
0.7	5.78140	5.84451	5.766942	127.453	128.156	127.4243	228.383	228.903	226.8065
0.8	4.81267	4.85699	4.796181	108.948	110.932	108.9018	203.312	203.924	199.8549
0.9	4.12690	4.18535	4.113669	96.7814	97.9970	96.75008	183.198	183.728	183.5335
1	3.67188	3.71927	3.656121	86.9989	88.4552	86.98845	167.351	168.052	165.5156

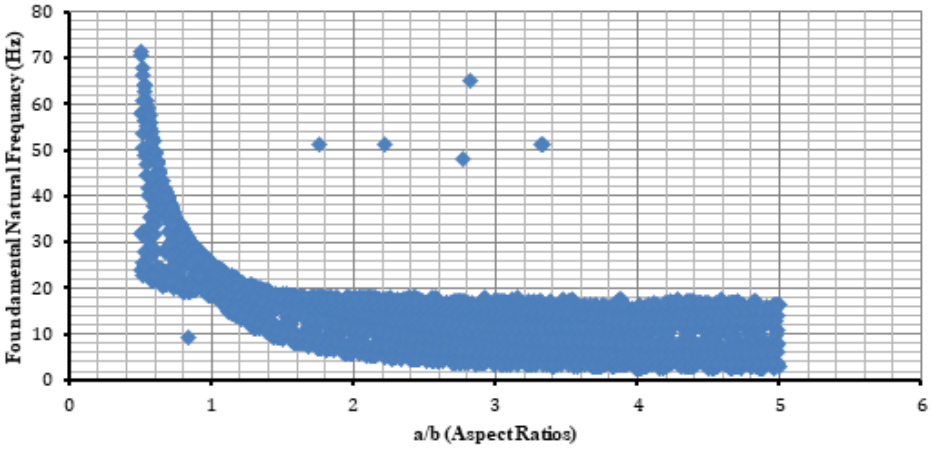

Fig. 2. Fundamental natural frequency versus the aspect ratios

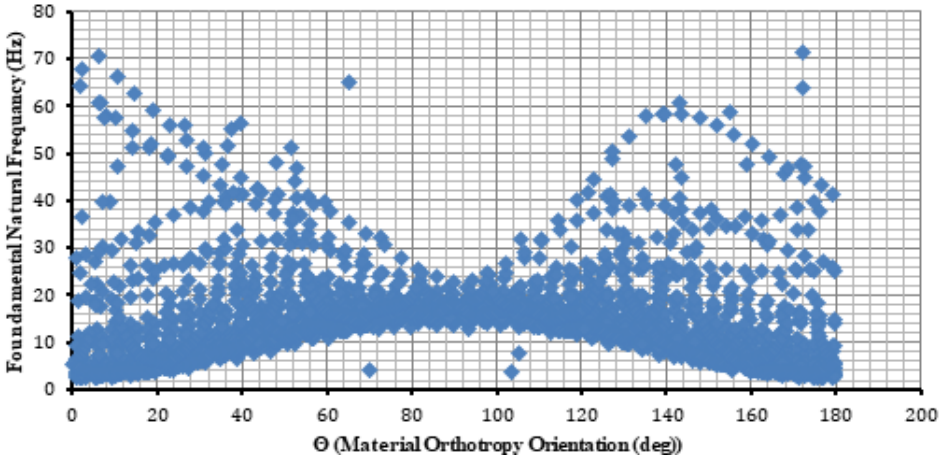

Fig. 3. Fundamental natural frequency versus the material orthotropy orientation

At roughness values close to zero, the slope of this diagram is too sharp; but as the roughness values increase, the critical force of movement approaches a constant number; thus, this parameter is very sensitive at near-zero values, and from values in the vicinity of 2, its sensitivity diminishes considerably.

In view of Fig. 3, the material orthotropy orientation can be introduced as the second sensitive parameter after aspect ratios. With the increase of this parameter, first the fundamental natural frequency increases and then decreases, with a sharp, albeit milder, slope relative to aspect ratios.

The diagram of the fundamental natural frequency versus depth of the fluid ratios has been shown in Fig. 4 with a positive, and near zero, slope. With the change of depth of the fluid ratios in its range of variations, a minor change is observed in the fundamental natural frequency, and so this parameter is not considered as a sensitive parameter for the fundamental natural frequency. Figure 5 shows the fundamental natural frequency versus the thickness ratios parameter. The parameter of thickness ratios is an input parameter with negligible effects on the fundamental natural frequency; and with the changes of this parameter in its relevant intervals, no tangible change is observed in the fundamental natural frequency.

The diagram of the fundamental natural frequency versus width of the tank has been shown in Fig. 6 with a near-zero slope. With the change of width of the tank in its range of variations, a minor change is observed in the fundamental natural frequency, and so this parameter is not considered as a sensitive parameter for the fundamental natural frequency.

Figure. 7 shows the percent sensitivity of fundamental natural frequency to parameters of aspect ratios, material orthotropy orientation, depth of the fluid, thickness ratios and width of the tank, which have been obtained by means of the EFAST method. According to this figure, the aspect ratios parameter (with 70% sensitivity) is the most important parameter, and the material orthotropy orientation (with 25% sensitivity) is the other effective parameter.

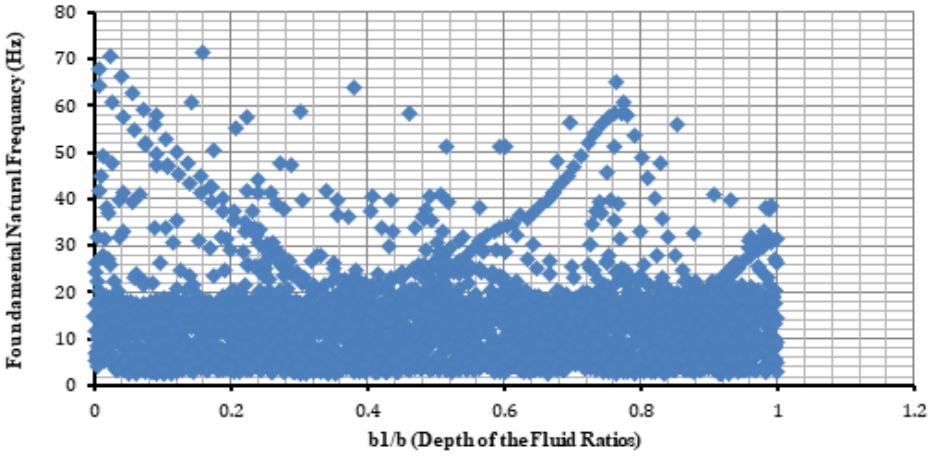

Fig. 4. Fundamental natural frequency versus depth of the fluid ratios

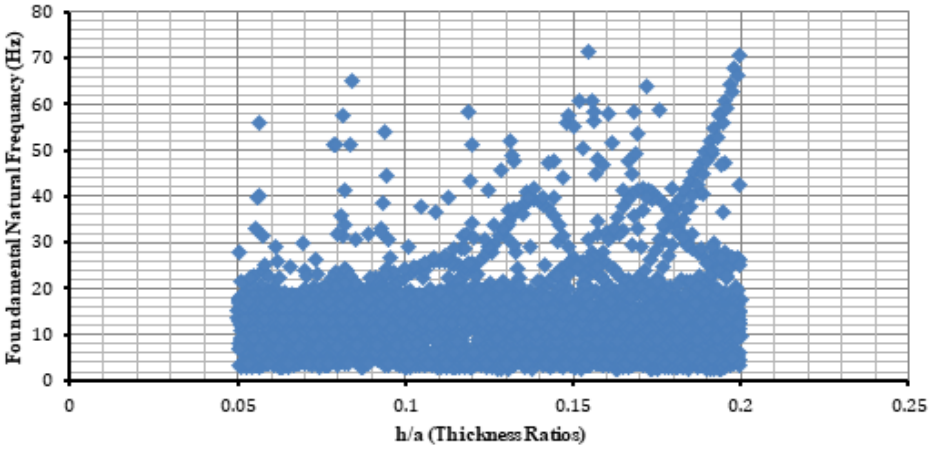

Fig. 5. Fundamental natural frequency versus the thickness ratios parameter

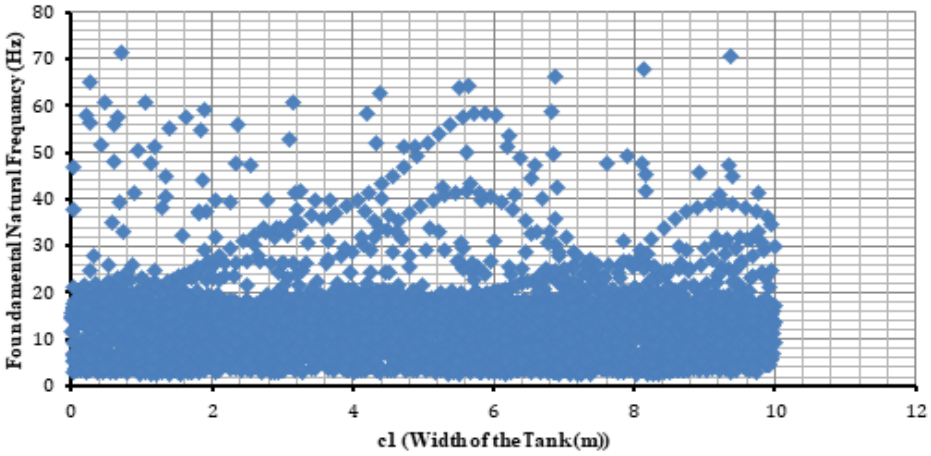

Fig. 6. Fundamental natural frequency versus width of the tank

7. Conclusions

In the present paper, sensitivity analysis of vibrating laminated composite rectangular plates in interaction with inviscid fluid has been presented. For the formulation, the modified higher order shear deformation plate theory is employed. Differential equations of motion were derived using Hamilton's variational principle. Natural frequencies of the plate were calculated using the Galerkin's method and the boundary conditions of the plate was simply supported. For sensitivity analysis, the EFAST model was utilized. This method was based on variance and it was independent of any assumption of linearity and uniformity between inputs and output(s).

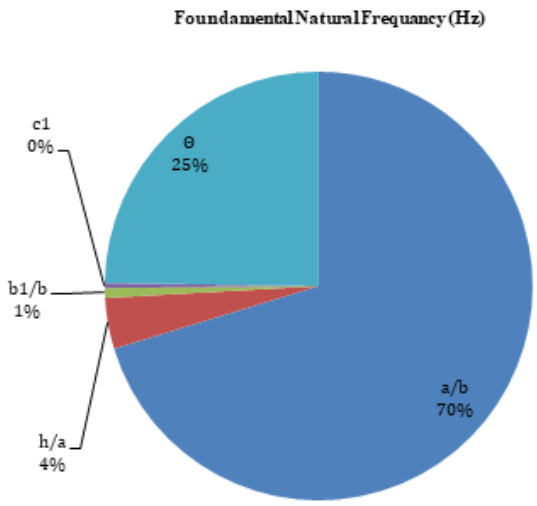

Fig. 7. Percent sensitivity of fundamental natural frequency to parameters

The EFAST model was used to qualitative and quantitative analysis of the effect of 5 parameters includes aspect ratio (a/b), thickness ratio (h/a), material orthotropy orientation (θ), depth of the fluid ratio (b_1 / b) and width of the tank (c_1) on the natural frequency of plate. It was observed that the aspect ratios parameter (with 70% sensitivity) was the most important parameter and after that material orthotropy orientation (with 25% sensitivity) was the second effective parameter on the natural frequency of plate. Also, results showed that other parameters such as thickness ratio and depth of the fluid ratio did not have a significant effect with 4% and 1% sensitivity respectively. Finally, the width of the tank with 0% did not have any effect on the natural frequency of the plate.

Acknowledgements

The authors gratefully acknowledge the funding by Arak University, under grant No 97/5115.

References

[1] Khorshidi K, Bakhsheshy A. Free vibration analysis of a functionally graded rectangular plate in contact with a bounded fluid. *Acta Mechanica* 2015; 226(10): 3401-23.

[2] Khorshid K, Farhadi S. Free vibration analysis of a laminated composite rectangular plate in contact with a bounded fluid. *Composite structures* 2013; 104: 176-86.

[3] Khorshidi K, Akbari F, Ghadirian H. Experimental and analytical modal studies of vibrating rectangular plates in contact with a bounded fluid. *Ocean Engineering* 2017; 140: 146-54.

[4] Yildizdag ME, Ardic IT, Demirtas M, Ergin A. Hydroelastic vibration analysis of plates partially submerged in fluid with an isogeometric FE-BE approach. *Ocean Engineering* 2019; 172: 316-29.

[5] Khorshidi K, Bakhsheshy A. Free natural frequency analysis of an FG composite rectangular plate coupled with fluid using Rayleigh–Ritz method. *Mechanics of Advanced Composite Structures* 2014; 1(2): 131-43.

[6] Omiddezyani S, Jafari-Talookolaei R-A, Abedi M, Afrasiab H. The size-dependent free vibration analysis of a rectangular Mindlin microplate coupled with fluid. *Ocean Engineering* 2018; 163: 617-29.

[7] Liao C-Y, Wu Y-C, Chang C-Y, Ma C-C. Theoretical analysis based on fundamental functions of thin plate and experimental measurement for vibration characteristics of a plate coupled with liquid. *Journal of Sound and Vibration* 2017; 394: 545-74.

[8] Carra S, Amabili M, Garziera R. Experimental study of large amplitude vibrations of a thin plate in contact with sloshing liquids. *Journal of Fluids and Structures* 2013; 42: 88-111.

[9] Jeong K-H, Kim K-J. Hydroelastic vibration of a circular plate submerged in a bounded compressible fluid. *Journal of Sound and Vibration* 2005; 283(1-2): 153-72.

[10] Khorshidi K. Effect of Hydrostatic Pressure on vibrating rectangular plates coupled with fluid. *Scientia Iranica Transaction A, Civil Engineering* 2010; 17(6): 415.

[11] Tubaldi E, Amabili M. Vibrations and stability of a periodically supported rectangular plate immersed in axial flow. *Journal of Fluids and Structures* 2013; 39: 391-407.

[12] Carra S, Amabili M, Ohayon R, Hutin PM. Active vibration control of a thin rectangular plate in air or in contact with water in presence of tonal primary disturbance. *Aerospace Science and Technology* 2008; 12(1): 54-61.

[13] Jeong K-H. Hydroelastic vibration of two annular plates coupled with a bounded compressible fluid. *Journal of fluids and structures* 2006; 22(8): 1079-96.

[14] Khorshidi K. Effect of hydrostatic pressure and depth of fluid on the vibrating rectangular plates partially in contact with a fluid. In: Proceedings of the.: Trans Tech Publ.

[15] Khorshidi K, Bakhsheshy A. Free Vibration analysis of Functionally Graded Rectangular plates in contact with bounded fluid. *Modares Mechanical Engineering* 2014; 14(8): 165-73.

[16] Ghasemi AR, Meskini M. Free vibration analysis of porous laminated rotating

circular cylindrical shells. *Journal of Vibration and Control* 2019: 1077546319858227.
[17] Ghasemi AR, Mohandes M, Dimitri R, Tornabene F. Agglomeration effects on the vibrations of CNTs/fiber/polymer/metal hybrid laminates cylindrical shell. *Composites Part B: Engineering* 2019; 167: 700-16.
[18] Mohandes M, Ghasemi AR. A new approach to reinforce the fiber of nanocomposite reinforced by CNTs to analyze free vibration of hybrid laminated cylindrical shell using beam modal function method. *European Journal of Mechanics-A/Solids* 2019; 73: 224-34.
[19] Ghasemi AR, Mohandes M. Nonlinear free vibration of laminated composite Euler-Bernoulli beams based on finite strain using generalized differential quadrature method. *Mechanics of Advanced Materials and Structures* 2017; 24(11): 917-23.
[20] Pianosi F, Beven K, Freer J, Hall JW, Rougier J, Stephenson DB, et al. Sensitivity analysis of environmental models: A systematic review with practical workflow. *Environmental Modelling & Software* 2016; 79: 214-32.
[21] Khedmati MR, Edalat P, Javidruzi M. Sensitivity analysis of the elastic buckling of cracked plate elements under axial compression. *Thin-Walled Structures* 2009; 47(5): 522-36.
[22] Afonso SMB, Hinton E. Free vibration analysis and shape optimization of variable thickness plates and shells—II. Sensitivity analysis and shape optimization. *Computing Systems in Engineering* 1995; 6(1): 47-66.
[23] Akoussan K, Boudaoud H, Koutsawa Y, Carrera E. Sensitivity analysis of the damping properties of viscoelastic composite structures according to the layers thicknesses. *Composite Structures* 2016; 149: 11-25.
[24] Chen C-S, Tan A-H. Imperfection sensitivity in the nonlinear vibration of initially stresses functionally graded plates. *Composite Structures* 2007; 78(4): 529-36.
[25] Fung C-P, Chen C-S. Imperfection sensitivity in the nonlinear vibration of functionally graded plates. *European Journal of Mechanics-A/Solids* 2006; 25(3): 425-36.
[26] Chen C-S, Hsu C-Y. Imperfection sensitivity in the nonlinear vibration oscillations of initially stressed plates. *Applied mathematics and computation* 2007; 190(1): 465-75.
[27] Łasecka-Plura M, Lewandowski R. Sensitivity Analysis of Dynamic Characteristics of Composite Beams with Viscoelastic Layers. *Procedia engineering* 2017; 199: 366-71.
[28] Kotełko M, Lis P, Macdonald M. Load capacity probabilistic sensitivity analysis of thin-walled beams. *Thin-Walled Structures* 2017; 115: 142-53.
[29] De Lima AMG, Faria AW, Rade DA. Sensitivity analysis of frequency response functions of composite sandwich plates containing viscoelastic layers. *Composite Structures* 2010; 92(2): 364-76.
[30] Takezawa A, Kitamura M. Sensitivity analysis and optimization of vibration modes in continuum systems. *Journal of Sound and Vibration* 2013; 332(6): 1553-66.
[31] Li Y, Wang X, Zhang H, Chen X, Xu M, Wang C. An interval algorithm for sensitivity analysis of coupled vibro-acoustic systems. *Applied Mathematical Modelling* 2017; 50: 394-413.
[32] Li D, Liu Y. Three-dimensional semi-analytical model for the static response and sensitivity analysis of the composite stiffened laminated plate with interfacial imperfections. *Composite Structures* 2012; 94(6): 1943-58.
[33] Li D-h, Xu J-x, Qing G-h. Free vibration analysis and eigenvalues sensitivity analysis for the composite laminates with interfacial imperfection. *Composites Part B: Engineering* 2011; 42(6): 1588-95.
[34] Liu Q. Analytical sensitivity analysis of frequencies and modes for composite laminated structures. *International Journal of Mechanical Sciences* 2015; 90: 258-77.
[35] Hu Z, Su C, Chen T, Ma H. An explicit time-domain approach for sensitivity analysis of non-stationary random vibration problems. *Journal of Sound and Vibration* 2016; 382: 122-39.
[36] Yan K, Cheng G. An adjoint method of sensitivity analysis for residual vibrations of structures subject to impacts. *Journal of Sound and Vibration* 2018; 418: 15-35.
[37] Choi M-S, Byun J-H. Sensitivity analysis for free vibration of rectangular plate. *Journal of Sound and Vibration* 2013; 332(6): 1610-25.
[38] Liu Q, Paavola J. General analytical sensitivity analysis of composite laminated plates and shells for classical and first-order shear deformation theories. *Composite Structures* 2018; 183: 21-34.
[39] Li DH, Liu Y, Zhang X. Linear statics and free vibration sensitivity analysis of the composite sandwich plates based on a layerwise/solid-element method. *Composite Structures* 2013; 106: 175-200.

[40] Tong C. Self-validated variance-based methods for sensitivity analysis of model outputs. *Reliability Engineering & System Safety* 2010; 95(3): 301-9.
[41] Nossent J, Elsen P, Bauwens W. Sobol'sensitivity analysis of a complex environmental model. *Environmental Modelling & Software* 2011; 26(12): 1515-25.
[42] Im S. Sensitivity estimates for nonlinear mathematical models. *Math Model Comput Exp* 1993; 1(4): 407-14.
[43] Sobol I. Sensitivity estimates for nonlinear mathematical models, Mater. Model; 1990.
[44] Cukier RI, Levine HB, Shuler KE. Nonlinear sensitivity analysis of multiparameter model systems. *Journal of computational physics* 1978; 26(1): 1-42.
[45] Saltelli A, Tarantola S, Chan K-S. A quantitative model-independent method for global sensitivity analysis of model output. *Technometrics* 1999; 41(1): 39-56.
[46] Homma T, Saltelli A. Importance measures in global sensitivity analysis of nonlinear models. *Reliability Engineering & System Safety* 1996; 52(1): 1-17.